TRANSNAV
http://www.transnav.eu
the International Journal on Marine Navigation and Safety of Sea Transportation
Volume 19
Number 1
March 2025

DOI: 10.12716/1001.19.01.10

Leveraging Radar and VTS for Enhanced Oil Spill Detection

M. Fiorini[1] & R. Trevisani[2]
[1] *Leonardo s.p.a, Roma, Italy*
[2] *GEM elettronica, San Benedetto del Tronto (AP), Italy*

ABSTRACT: The Norwegian Clean Seas Association for Operating Companies (NOFO) conducted oil-on-water exercises in 2018 to evaluate new oil spill response technologies, including advanced radar systems. This study assesses radar performance based on data collected during these exercises, focusing on the potential of radar technology to enhance Vessel Traffic Services (VTS) systems. By analysing radar data from various simulated oil spill scenarios, key strengths, weaknesses, and areas for improvement were identified. Findings highlight the benefits of integrating radar technology into VTS for improved oil spill detection, tracking, and response. This includes recommendations for expanding VTS system features to leverage radar data more effectively, such as developing algorithms for automated oil spill detection and implementing real-time data fusion techniques. The study demonstrates the potential of radar- enhanced VTS systems to significantly improve oil spill response capabilities, particularly in challenging conditions.

1 INTRODUCTION

The integration of radar technology with Vessel Traffic Services (VTS) significantly enhances the detection and management of oil spills. Radar systems offer direct detection capabilities by identifying changes in radar backscatter caused by oil on the water surface. Oil spill on the sea surface dampens the sea clutter observed by the radar. This is a result of dampening of the wind generated capillary wave [1]. The suppression of capillary waves by oil slicks creates characteristic "dark spots" on radar images, serving as potential spill indicators. Additionally, within the VTS framework, radar indirectly aids in oil spill detection by monitoring vessel movements and identifying any unusual behaviour that might suggest a spill incident.

VTS centres play a crucial role in disseminating information about potential oil spills. When radar systems detect anomalies indicative of a spill, VTS networks relay this information to relevant authorities. Similarly, reports from vessels about oil spills are rapidly disseminated through the VTS system. Furthermore, VTS facilitates traffic management during oil spill response operations. This includes rerouting vessels to avoid the spill area, establishing exclusion zones to protect the environment and facilitate cleanup efforts, and streamlining coordination with other responders.

The integration of radar data with VTS systems provides a more comprehensive situational awareness during oil spill response. For example, if radar detects an oil slick, VTS data can help identify potential source vessels in the vicinity. This integration also contributes to faster response times by enabling rapid generation and dissemination of alerts.

Prompt detection and monitoring of oil spills in the marine environment are critical for effective environmental protection and response strategies.

Spilled oil rapidly spreads across the water surface, forming a toxic film that disrupts oxygen exchange and severely harms aquatic ecosystems. Early detection is vital for enacting containment measures and mitigating the long-term impacts on marine life, ecosystems, and local communities.

This paper presents a comparative analysis of X-band and Ka-band radar systems, focusing on their efficacy in detecting oil spills on the sea surface. However, it is important to acknowledge that radar-based oil spill detection has limitations, as it can be influenced by factors such as weather conditions, sea state, and the features of the oil film.

2 SATELLITE VERSUS LAND/SHIP-BASED RADAR

Satellite-based radar, particularly Synthetic Aperture Radar (SAR) such as the European Space Agency (ESA), COSMO-SkyMed Series, [2], has been extensively employed for the detection of oil spills from space. SAR technology is valued for its ability to provide high spatial resolution imagery that is independent of range, while operating effectively under all weather conditions and during both day and night. This capability enables the remote and near real-time monitoring of marine oil spills, which is critical for prompt emergency response and environmental protection, especially in regions where direct on-site assessment is impractical.

The detection of oil spills by SAR is achieved through the identification of dark patches on the sea surface, which result from the damping effect of oil on capillary waves. These dark areas contrast with the surrounding sea clutter, allowing for the delineation of oil-contaminated zones. However, the presence of natural look-alikes, such as areas of low wind or biogenic films, may lead to false positive detections, [3]. Consequently, advanced image processing and classification techniques have been developed to improve the accuracy of spill identification.

Despite its advantages, SAR detection is subject to certain limitations. The effectiveness of detection is influenced by sea state and wind conditions, with optimal performance observed at wind speeds ranging from approximately 1.5 m/s to 6 m/s (i.e. Beaufort Sea State up to 3). At wind speeds below this range, the contrast between oil and the sea surface diminishes, while higher wind speeds cause increased scattering of radar signals, thereby reducing detection capability, [3]. Additionally, the temporal resolution of satellite-based radar is constrained by satellite revisit intervals, although recent developments in satellite constellations have sought to address this limitation.

Recent advances have been made through the integration of machine learning and deep learning algorithms with SAR imagery, resulting in enhanced detection accuracy and speed. Automated and robust identification of oil spills from satellite data has thus been increasingly realized, [4].

In contrast, land-based and shipborne radars, commonly operating within the X-band frequency, have been utilized for oil spill detection at closer ranges, typically up to 24 NM at the very latest. These radar systems can be adjusted to mitigate sea clutter effects and have demonstrated success in detecting surface slicks, particularly in coastal and port environments.

The deployment of shipborne radar offers flexibility for targeted monitoring and can serve as a complementary tool to satellite data by providing higher temporal resolution and immediate local surveillance. Furthermore, such systems are generally less costly and can be rapidly deployed in response to spill events.

However, the detection range of land and ship-based radars is inherently limited by their lower altitude relative to satellites. Similar to satellite radar, environmental conditions such as sea state and wind speed impose constraints on detection capability. Moreover, the spatial coverage of these systems is substantially narrower, and their operation may require manual control or integration with additional sensors to ensure effective monitoring.

A comparative analysis reveals that satellite-based radar systems provide extensive coverage ranging from regional to global scales, with high spatial resolution that remains consistent regardless of range. Temporal resolution, however, is limited by satellite revisit times.

Conversely, land and ship-based radars offer continuous local monitoring with higher temporal resolution but are restricted in spatial coverage. Both systems exhibit robustness to weather conditions, though detection efficacy is optimal under moderate wind speeds.

From a cost and deployment perspective, satellite infrastructure entails higher expenses, whereas land and ship-based radar systems are comparatively economical and more flexible in deployment.

Table 1. Comparative summary

Aspect	Satellite-Based Radar (SAR)	Land/Ship-Based Radar
Coverage Area	Very large, regional to global	Limited to coastal or local areas
Spatial Resolution	High, range-independent	Moderate, depends on antenna and altitude
Temporal Resolution	Limited by satellite revisit times	High, continuous local monitoring possible
Weather Independence	Operates in all weather and lighting conditions	Affected by weather but generally robust
Sea State Sensitivity	Optimal detection at moderate wind speeds (1.5-6 m/s)	Similar constraints as satellite radar
Cost and Deployment	High cost, requires satellite infrastructure	Lower cost, flexible deployment on ships/land
Detection Accuracy	High with advanced processing and ML integration	Good, but limited by range and environmental conditions
Use Case	Large-scale monitoring, emergency response, pollution source identification	Local monitoring, spill tracking, complementary to satellite data

To summarise, satellite-based SAR remains the preeminent technology for large-scale, all-weather oil spill detection due to its broad coverage and high spatial resolution, making it indispensable for initial spill identification and ongoing monitoring. Nevertheless, its temporal resolution is limited by orbital parameters. Land and ship-based radar systems provide valuable complementary capabilities, offering enhanced temporal resolution and localized flexibility, albeit with range and environmental limitations.

3 NOFO OPV EXERCISE

This study is based on data collected during the Norwegian Oil on Water (NOFO OPV) exercise conducted on the Frigg field in Norway in 2018 (Figure 1). The NOFO OPV, a biennial exercise conducted in collaboration between the Norwegian Coastal Administration and the Norwegian Clean Seas Association for Operating Companies (NOFO), is unique in its use of actual oil releases. This allows for realistic testing of the latest technologies for remote sensing, containment, and recovery of oil spills, attracting international participation and attention. More than 10 cooperating units (Table 2), including both aerial and naval assets, were involved in the exercise activities.

Figure 1. NOFO OPV 2018 Exercise Area (Image from EMODnet: European Marine Observation and Data Network)

Table 2. OPV 2018 principal operating units [5]

Name	Type	Role
KV Sortland	Patrol Vessel	Oil discharge, Remote Sensing Exercise Command and Safety
Strillborg	Offshore Supply Vessel	Experiment with In- Situ Burning Oil
Torsborg	Offshore Supply Vessel	Experiment with Oil, Recovery System, (MOS Sweeper 50)
OV Utvær	Pollution Control Vessel	Exercise Safety
Siem Symphony	Offshore Supply Vessel	Experiment with Oil Containment Boom (Spillraider 1200s)
Bøen	Trawler	Oil Spill Protection
Vestbris	Trawler	Oil Spill Protection
Midnight 01 (LN- KYV)	Aircraft	Remote Sensing
Finnguard 01	Aircraft	Remote Sensing
Swecoast 503	Aircraft	Remote Sensing

The 2018 exercise was carried out on the Frigg field, a decommissioned gas field in the North Sea that provides a suitable environment for controlled oil spill experiments, in an area within 10 NM of the position 59° 59′ 00″ N, 002° 27′ 00″ E.

On the first day (June 6th, 2018), a total volume of 72 m^3 oil emulsion was discharged into the area. The emulsion was released directly in front of the recovery system at a distance of approximately 300 m. Part of the oil spill was recovered, and the other part was dispersed into the environment, creating a long streak of oil on the sea surface. The spill was followed by recovery operations utilizing oil skimmer systems and oil containment booms. Recovery and oil dispersion activities continued into the second day (June 7th, 2018). Marine weather conditions remained stable throughout the two-day trial, with mean wind speeds ranging from 16 to 21 knots and wind directions predominantly from north to north-northeast (N-NNE). The experience at NOFO OPV 2018 highlighted both the advantages and disadvantages of these systems and the effect of radar characteristics and parameters on the outcomes.

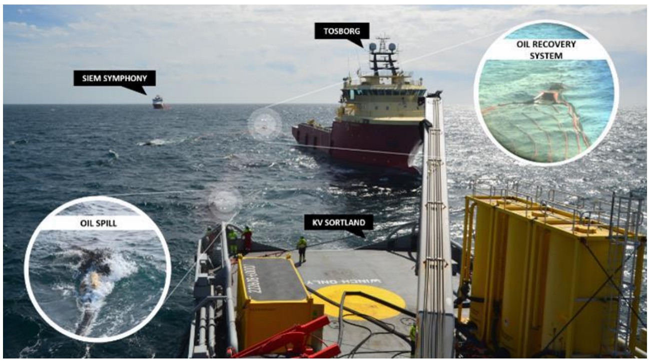

Figure 2. OFO OPV 2018 Oil Discharge Scenario From KV SORTLAND

3.1 *Spilled Oil Properties*

The 2018 NOFO OPV exercise utilized a specially formulated oil emulsion derived from evaporated Oseberg Blend crude oil. This specific crude oil was chosen due to NOFO's extensive experience in creating emulsions with it. While the composition of Oseberg Blend can fluctuate slightly based on production rates, it is generally classified as a light, paraffinic crude oil with a density of approximately 840 g/l.

To simulate the weathering process of oil on water, the Oseberg Blend was evaporated at temperatures exceeding 200°C. This evaporation process aimed to replicate the characteristics of oil that has been exposed to the marine environment for roughly one day, creating a more realistic scenario for the exercise.

To create a stable oil emulsion for the NOFO OPV exercise, a specific mixing ratio was used:

- Up to 40% evaporated Oseberg Blend: This forms the base of the emulsion.
- Up to 10% tungsten (IF 380): Tungsten was added to increase the emulsion's density, making it easier to observe and track in the water.
- Minimum 50% seawater: Seawater is the primary emulsifying agent, helping to disperse the oil and create a stable mixture.

This formulation builds upon previous exercises. The 2018 OPV emulsion was largely reused from the 2016 exercise. However, due to the hydrogen sulphide (H2S) that can accumulate in stored seawater emulsions, up to 10 litres of H2S remover were added to ensure the safety and quality of the emulsion [5].

Table 3. Oseberg Blend Properties [6]

Whole Crude Properties	
Density @ 15°C (g/cc)	0,827
API Gravity	39,6
Total Sulphur (% wt)	0,20
Pour Point (°C)	-15
Viscosity @ 20°C (cSt)	4,14
Viscosity @ 40°C (cSt)	2,70

4 DUAL BAND RADAR SYSTEM

The GEMINI-DB radar system, produced by GEM Elettronica (an Italian company controlled by Leonardo s.p.a.), was installed on one of the cooperating vessels and deployed during the NOFO OPV trial on both June 6th and June 7th. This dual-band radar, operating in both X-band and Ka-band, is designed to provide enhanced situational awareness in the surveillance of infrastructures and is particularly well-suited for detecting oil spills in challenging maritime environments. The combination of X-band and Ka-band allows the GEMINI-DB to overcome the limitations of each individual band, providing both high sensitivity to small oil spills at short ranges (Ka-band) and robust performance in challenging weather conditions and at longer ranges (X-band).

Table 4. GEMINI-DB System Characteristics

System Characteristics	Ka-band Radar	X-band Radar
Radar Technology	Pulsed Magnetron Radar	Pulsed Doppler Radar
Transmitter Type	Magnetron / Non-Coherent	Solid State / Coherent
Transmitter Peak Power	10 kW	400W
Frequency GHz	[33.600:34.100] [9.300:9.500] GHz	
Antenna Gain	40 dB	31 dB
Antenna Polarization	Circular	Horizontal
Antenna Horizontal Beamwidth at -3dB	< 0.3°	< 0.9°

Figure 3. GEM GEMINI-DB X-Ka Dual Band Radar System

The X-band radar employs pulsed Doppler technology with solid-state transmitters, whereas the Ka- band radar uses pulsed radar technology based on magnetron. The lower frequency of the X-band results in reduced clutter return, enabling more efficient filtering of external disturbances caused by waves and rain.

The Ka-band radar, due to its millimeter-wavelength operation, is significantly more sensitive to the scattering of very small objects, such as raindrops and wind-induced facets on the sea surface providing higher sensitivity for detecting the subtle changes in backscatter caused by oil. The Ka-band's use of circular polarization partially mitigates its limitations in rain and enhances its detection capabilities for depolarizing objects.

On the other hand, the X-band excels at medium to high ranges, higher sea states, and poor meteorological conditions due to its lower frequency. This broader operational capability of the X-band aligns with its adoption as the standard for navigation radar under IMO regulations.

A very first version of the GEMINI-DB radar system with a non-coherent transceiver was deployed during NATO Harbour Protection Trials 2008 hosted in Eckernförde, Germany, demonstrating its versatility in diverse surveillance applications.

The concept behind this radar system is to combine the strengths of both bands: Ka-band for improved small target detection at short range and X-band for longer detection ranges and better clutter rejection, making it a valuable tool for oil spill detection and response [7].

4.1 *Radar Installation and Data Acquisition*

The GEMINI-DB dual-band radar was temporarily installed on the Norwegian Coast Guard patrol vessel KV Sortland at a height of 19 meters above the waterline.

The radar's radiating sector was positioned on the port side of the ship, covering an area of approximately 210 degrees.

This configuration allowed for comprehensive surveillance of the oil spill area during the NOFO OPV exercise.

Figure 4. GEM GEMINI-DB radiation sector on KV SORTLAND offshore patrol vessel

During the trials, the following data were recorded:

- X-band raw signal (digitalized): This provides the raw data from the X-band radar, capturing the backscattered signals from the sea surface and any potential oil spills.
- Ka-band raw signal (digitalized): Similar to the X-band data, this records the raw signal from the Ka-band radar, offering higher sensitivity for detecting smaller oil spills.
- GPS data (Latitude/Longitude/Course Over Ground/Speed Over Ground @ 1 Hz frequency): This provides precise information about the vessel's position and movement, which is crucial for accurately geo-referencing the radar data and tracking the oil spill's location.
- Gyrocompass data (Heading/Roll/Pitch @ 10 Hz frequency): This data captures the vessel's orientation and motion in detail, allowing for compensation of any movements that might affect the radar measurements.

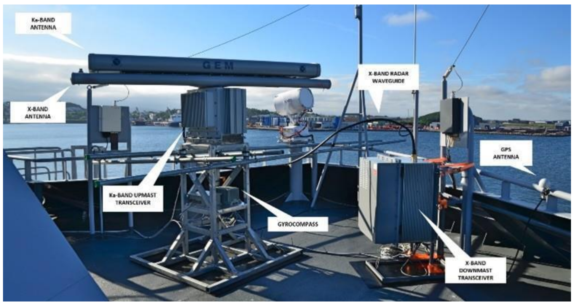

Figure 5. GEM GEMINI-DB Radar System installation on KV SORTLAND offshore patrol vessel

A total period of 19 hours with oil-on-water was recorded, providing a substantial dataset for analysing the performance of the GEMINI-DB radar in detecting and tracking oil spills under various conditions.

Additionally, GEM elettronica Oil Spill Detector (OSD) elaborator was installed on board KV SORTLAND to process radar and navigation data for the automatic extraction of oil spill tracks. The GEM OSD software supported oil spill dispersion operations during the whole trial. An image of the graphical user interface is shown in Figure 6.

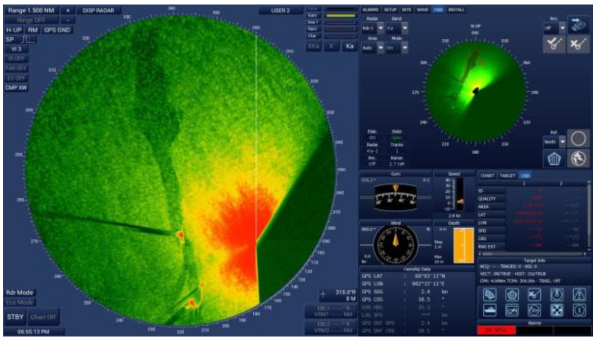

Figure 6. Screenshot of the graphical user interface of GEM Oil Spill Detector (OSD) software

Such information should be shared from ship to shore, enabling the VTS or, more generally, the shore-side center of the eNavigation, to fulfill one of its core mission: the protection of the maritime environment, [8].

Vessel Traffic Services (VTS) and Coastal Surveillance Systems (CSS), [9], [10], are crucial for mitigating maritime oil spills, acting as essential components of marine safety and environmental protection.

Upon the detection of a potential spill, whether through advanced radar systems equipped with oil detection capabilities, visual observation, or reports from vessels in the vicinity, the eNavigation shore-side center acts as the first responder. Their immediate action involves alerting the appropriate emergency response teams, including specialized pollution cleanup crews with expertise in containment and recovery, relevant environmental agencies responsible for assessing ecological damage and coordinating long-term remediation efforts, and port authorities who manage harbor operations and ensure the safety of port facilities. This rapid notification process is critical in minimizing the time it takes to initiate an effective response, thereby reducing the spread and impact of the spill.

The eNavigation shore-side operators then coordinate the complex and multifaceted response efforts that follow, which may include directing vessels involved in the cleanup operation to the precise location of the spill using real-time tracking and communication systems. They also provide crucial navigational assistance to these vessels, guiding them through potentially hazardous conditions and ensuring the safe and efficient deployment of containment booms, skimmers, and other specialized equipment to contain the spill's spread. This optimized vessel positioning is essential for maximizing the effectiveness of the cleanup operation.

Simultaneously, the eNavigation shore-side continuously monitors the movement of the oil spill, utilizing predictive models and real-time data to forecast affected areas and inform the development of dynamic response strategies. This continuous monitoring allows response teams to adapt their tactics as the situation evolves, ensuring that efforts remain focused and effective, and minimizing the overall environmental damage.

The eNavigation shore-side center also serves as a central hub for information exchange, providing updates to all stakeholders, including government agencies, industry representatives, and the public, ensuring transparency and facilitating a coordinated response.

Furthermore, the eNavigation shore-side plays a vital role in ensuring the safety of navigation in the affected area, which is critical for preventing further incidents and protecting both the environment and human life.

Depending on the location and extent of the spill, the eNavigation shore-side will manage vessel traffic by providing early warnings to approaching ships, alerting them to the presence of the spill and potential hazards. They also establish temporary exclusion zones with clearly defined boundaries to prevent further contamination of the affected area and protect response personnel and equipment operating on-scene. Deviating shipping routes to guide vessels safely around the spill is another key function, ensuring that maritime traffic can continue to move efficiently while avoiding both direct contact with the oil and the potential for secondary incidents. This traffic management is not only critical for preventing secondary incidents, such as collisions or groundings that could exacerbate the situation and lead to further release of pollutants, but also for ensuring the efficient and safe movement of vessels in the vicinity, including those directly involved in the cleanup operation. The eNavigation shore-side center's comprehensive traffic overview and communication systems are indispensable for coordinating complex navigational maneuvers. The eNavigation shore- side leverages advanced technology and dynamic coordination to minimize both immediate and long-term environmental and economic damage from oil spills. Ultimately, the eNavigation shore- side ensures the safety, efficiency, and resilience of maritime operations in the face of such disasters.

5 RESULTS

The first processed oil spill radar images analysed were captured approximately two hours after the initiation of the OPV trial (Figure 7). During the oil emulsion release operation from KV Sortland, the vessel maintained an almost constant trajectory with a Course Over Ground (COG) of 10°T and a Speed Over Ground (SOG) of about 2 knots. After two hours, the oil emulsion release was stopped, allowing for observation of the full spatial extent of the oil streak within the radar's coverage area.

X-band and Ka-band radar images were time-integrated over a period of 1 minute to enhance the discrimination performance of the oil slick against sea clutter. Longer integration periods were not considered, as the navigation sensor errors associated with the ship's own motion compromise radar image stabilization, leading to performance degradation over extended integration times.

Figure 7 displays radar images of the oil spill: the Ka-band radar image is shown on the left, while the X-band radar image is on the right. A closer analysis reveals damping areas behind the targets illuminated by the radar. These sectorial areas result from beam shading effects caused by the physical dimensions of the targets obstructing the radar beam. If not properly managed, these areas may lead to false oil detections (false alarms). To mitigate this issue, automatic oil spill detection (OSD) processors typically apply sectorial inhibition masks behind the position of large targets. The tracks of these targets are, usually, provided to OSD systems by ARPA tracking systems or AIS receivers.

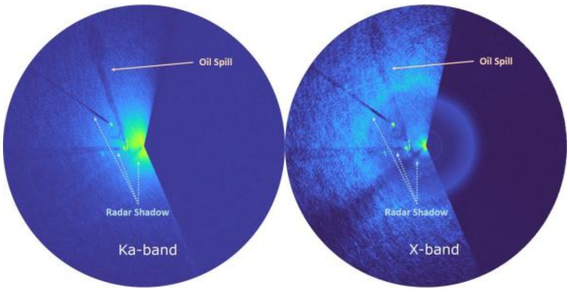

Figure 7. NOFO OPV 2018 Oil Spill PPI Radar Integrated Images (6 km range scale): Ka-band (left) and X-band (right)

Analysis of the integrated radar data revealed that the oil emulsion formed a long, narrow streak with a total range extent of about 5.5 kilometres. The width of the streak varied from 100 to 400 meters, resulting in a total affected surface area of approximately 1.98 km².

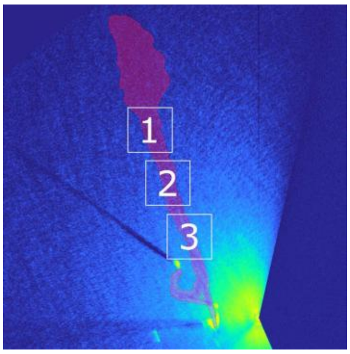

Figure 8. The three measurement areas superimposed on the oil spill shape polygon (Ka-band radar)

To evaluate the impact of the oil spill on the X-band and Ka-band radar signals, three measurement areas are selected within the spill region. These areas are positioned at different grazing angles.

To normalize the measurements from the two radars and assess the difference in damping over the oil slick, the mean clutter reflectivity, σ_0 , is considered.

The surface clutter cross section, σ_c (m²), of a patch defined by the intersection at the earth's surface of the azimuth beamwidth with a range gate at a range R (m) is calculated using the radar equation [11]:

$$\sigma_c = \frac{(4\pi)^3 R^4 P_r L F^4}{P_t G^2 G_{pc} \lambda^2}$$

where P_t is the transmitted peak power (W), P_r is the received power (W) from the surface clutter patch, G is the antenna gain, G_{pc} is the pulse compression gain, λ is the radar wavelength (m), F is the pattern propagation factor that incorporates the effects of the antenna pattern and the radar environment. L is a series of loss factors:

$$L = L_t \cdot L_q \cdot L_{bs} \cdot L_r^2 \cdot L_{r,m}$$

In which:
L_t is transmitter loss,
L_r is radome loss,
L_{bs} is antenna beamshape loss,
L_q is ADC quantisation loss,
$L_{r,m}$ is receiver mismatch loss.

The mean clutter reflectivity, σ_0, is then calculated from the clutter cross section, σ_c:

$$\sigma_0 = \frac{\sigma_c}{A}$$

In which A (m²) represents the area of the clutter patch, being the product of its width and its depth [12].

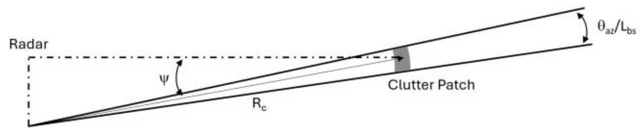

Figure 9. Clutter patch area

$$A = R_c \frac{\theta_{az} \cdot c \cdot \tau}{L_{bs} \cdot 2 \cdot \cos\psi}$$

where c is the speed of light (299792458 m/s), R_c is the ground range (m), ψ is the grazing angle, τ is the pulse width of the compressed pulse (s).

Figures 10, 11, and 12 show the radar received power (upper: Ka-band, lower: X-band) corresponding to observation areas 1, 2, and 3, respectively, from which the mean clutter reflectivity values are calculated.

The various damping measurements of the oil slick on capillary waves, measured using X- and Ka- band radars, were found to be generally consistent across the three observation areas and they are reported in Table 5.

In the first observation area, positioned at a grazing angle between 0.25° and 0.32°, the mean clutter reflectivity difference between the oil dumped area and the clean sea surface averaged -4.7 dB for the Ka-band, while the X-band radar exhibited a difference of -2.7 dB. In the second observation area, with a grazing angle between 0.32° and 0.44°, the mean clutter reflectivity difference for the Ka-band averaged -4.9 dB, whereas the X-band radar exhibited a difference of -2.5 dB. Finally, in the third observation area, positioned at a grazing angle between 0.45° and 0.85 °, the mean clutter reflectivity difference for the Ka-band averaged -4.8 dB, while the X-band radar exhibited a difference of -2.5 dB.

Table 5. measured average oil damping on sea clutter reflectivity

Area Number	Grazing Angles	Mean Clutter Reflectivity Difference on Oil Damping (Ka-band)	Mean Clutter Reflectivity Difference on Oil Damping (X-band)
1	0.25° to 0.32°	-4.7 dB	-2.7 dB
2	0.32° to 0.44°	-4.9 dB	-2.5 dB
3	0.45° to 0.82°	-4.8 dB	-2.5 dB

According the analysis, the X-band radar exhibited an average damping on the clutter reflectivity ranging from -2.5 dB to -2.7 dB, while the Ka-band radar showed a damping between -4.7 dB and -4.9 dB. Consequently, the Ka-band demonstrated an additional advantage ranging from -2 dB to -2.2 dB. It should be noted that this advantage was evaluated under the conditions recorded during the NOFO OPV 2018 trial, characterized by wind speeds between 16 and 21 knots and a thin oil film resulting from the utilized oil emulsion, [13].

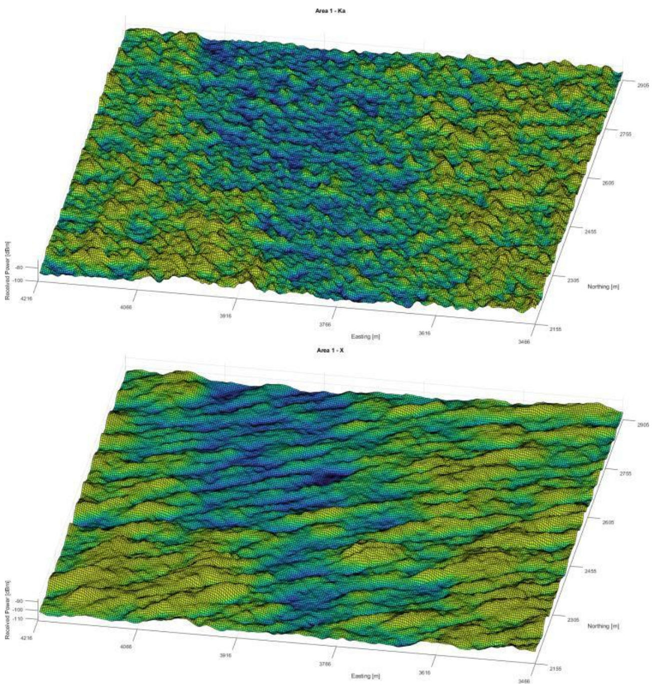

Figure 10. MEASUREMENT AREA 1 – Radar received power on sea surface affected by oil spill (Upper: Ka-band, Lower: X-band)

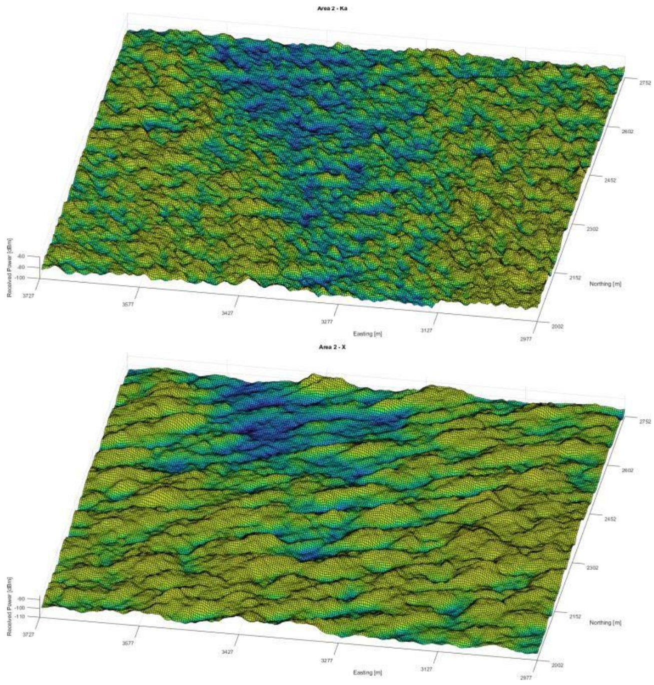

Figure 11. MEASUREMENT AREA 2 – Radar received power on sea surface affected by oil spill (Upper: Ka-band, Lower: X-band)

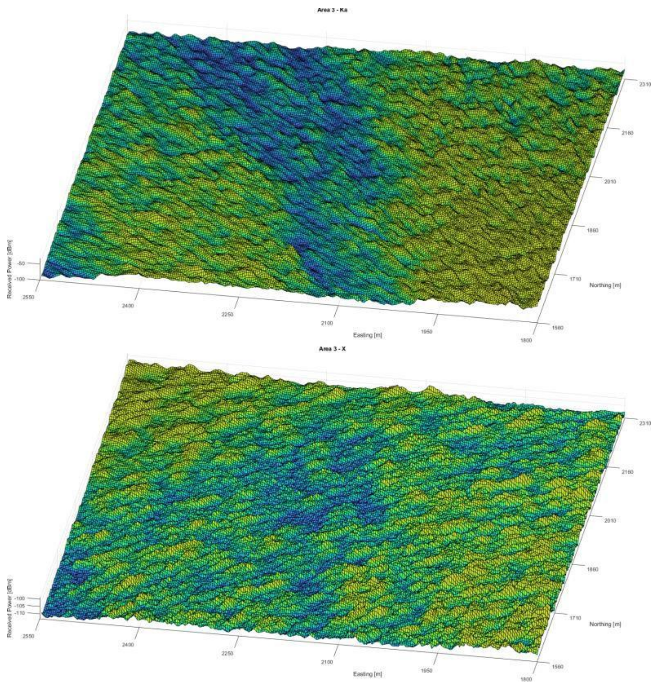

Figure 12. MEASUREMENT AREA 3 – Radar received power on sea surface affected by oil spill (Upper: Ka-band, Lower: X-band)

The differences observed between the two radars are not limited to the damping effect on the capillary waves by the oil spill. Additional differences emerge in their ability to discriminate thin oil streaks. This discrimination capability is strongly influenced by the higher resolution of the Ka-band radar, which proves to be one of the most critical parameters for this type of sensor designed for oil spill detection. These differences in discrimination are clearly visible in Figure 13, where it is reported the radar image (upper image: Ka-band, lower image: X-band) of the oil spill after about 22 hours after the oil emulsion release. Here, the Ka-band radar successfully distinguishes thin oil emulsion streaks as narrow as less than 15 meters.

These performance characteristics become particularly important as the oil spill evolves over time, causing its geometric shape to become less regular and more fragmented, with thin oil streaks emerging that are difficult to detect using low/medium resolution radar systems. Under these conditions, a high-resolution radar like the Ka-band radar used in this study enables more accurate and efficient execution of critical oil spill dispersion operations.

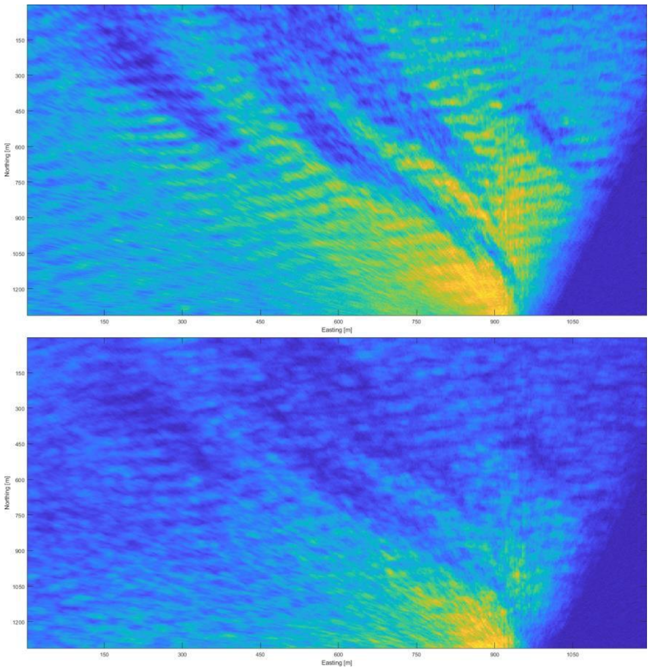

Figure 13. Differences on oil patches discrimination (Upper: Ka-band, Lower: X-band)

6 CONCLUSIONS

This study demonstrated that Ka-band radar outperforms X-band radar in oil spill detection during the NOFO OPV 2018 trial, offering higher contrast, finer resolution, and greater sensitivity to thin oil layers and capillary wave damping. Ka-band data showed nearly 2 dB greater sea clutter damping than X-band, confirming previous findings and enabling more precise spill delineation.

However, Ka-band's performance is limited by adverse weather conditions, where X-band radar remains more reliable. The complementary strengths of both bands, as integrated in the GEMINI-DB dual-band radar system, provide a robust, all-weather solution for vessel traffic service (VTS) operators, enhancing early spill detection and response.

Future work should develop automated detection algorithms, optimize dual-band parameters, and integrate radar with other sensors to further improve oil spill monitoring and environmental protection.

REFERENCES

[1] M. Fingas, Handbook of Oil Spill Science and Technology, Wiley, 2015.

[2] The European Space Agency (ESA), COSMO-SkyMed, https://earth.esa.int/eogateway/missions/cosmo-skymed

[3] Carl E. Brown, Merv F. Fingas, Mathias Fruhwirth and R. Lloyd Gamble, "Oil Spill Remote Sensing: A Brief Review of Airborne and Satellite Sensors", presented at the SPOT Image 1995 User Group Meeting, Washington, D.C., USA, 24-25 August, 1995, pp 1-14.

[4] Al-Ruzouq, Rami, Mohamed Barakat A. Gibril, Abdallah Shanableh, Abubakir Kais, Osman Hamed, Saeed Al-Mansoori, and Mohamad Ali Khalil. 2020. "Sensors, Features, and Machine Learning for Oil Spill Detection and Monitoring: A Review" Remote Sensing 12, no. 20: 3338. https://doi.org/10.3390/rs12203338

[5] Olje på Vann 2018, Weblink, https://www.nofo.no/globalassets/pdfs/opv2018_sluttrapport.pdf

[6] Crude Oil Assays, Weblink, https://www.statoil.com/en/what-we-do/crude-oil-and-condensate- assays.html

[7] Roberto Trevisani (GEM elettronica, Italy), Federico Principi (GEM elettronica, Italy). "Radar Systems and Processing Techniques for Improved Small Target Detection in Coastal and Maritime Scenarios". NATO Science for Peace and Security Series – D: Information and Communication Security. Volume 65: Modern Technologies Enabling Innovative Methods for Maritime Monitoring and Strengthening Resilience in Maritime Critical Infrastructures.

[8] Michele Fiorini and Natalie Gupta (editors), "ICT Solutions and Digitalisation in Ports and Shipping", The Institution of Engineering and Technology (IET) Transportation Series, ISBN 978-1-83953-086- 9, 1839530863, pp 460, London, 2021, Book DOI: 10.1049/PBTR030E

[9] M. Fiorini, "Acceptance test procedures for a national wider radar coastal surveillance system. The ZSRN experience", 4th IEEE Int. Workshop on Metrology for AeroSpace (MAS), ISBN 978-1-5090- 4233-3, Padua, Italy, 21-23 June 2017, pp. 26-31, INSPEC Accession Number: 17082234, DOI: 10.1109/MetroAeroSpace.2017.7999590

[10] M. Fiorini, S. Maciejewski, "Lesson learned during the realization of the automated radar control system for Polish sea-waters (ZSRN)", in "Advance in Marine Navigation – Marine Navigation and Safety of Sea Transportation" edited by Adam Weintrit, CRC Press, Balkema, The Netherlands, ISBN 978-1-138-00106-0, June 2013, pp. 217-221

[11] Maurice W Long, "Radar Reflectivity Of Land And Sea, Third Edition", Artech House, 2001.

[12] Albert G. Huizing, Arne Theil, "CARPET Version 3 User's Manual', TNO

[13] Stein Sandven (NERSC, Bergen, Norway), Vladimir Kudriavtsev (NIERSC, St. Petersburg, Russia) and Vladimir Malinovsky (MHI, Sevastopol, Ukraine). "Development of Marine Oil Spills/slicks Satellite monitoring System elements for the Black Sea, Caspian Sea and /Kara/Barents Seas". The 2nd international workshop on advances on SAR oceanography from ENVISAT and ERS mission. January 2008 – ESA ESRIN – Rome – Italy.